

VoroNav: Voronoi-based Zero-shot Object Navigation with Large Language Model

Pengying Wu^{1*} Yao Mu^{2,3*} Bingxian Wu¹ Yi Hou¹ Ji Ma¹
Shanghang Zhang^{1†} Chang Liu^{1†}

¹ Peking University ² The University of Hong Kong ³ OpenGVLab, Shanghai AI Laboratory
{shanghang, changliucoe}@pku.edu.cn

Abstract

In the realm of household robotics, the Zero-Shot Object Navigation (ZSON) task empowers agents to adeptly traverse unfamiliar environments and locate objects from novel categories without prior explicit training. This paper introduces VoroNav, a novel semantic exploration framework that proposes the Reduced Voronoi Graph to extract exploratory paths and planning nodes from a semantic map constructed in real time. By harnessing topological and semantic information, VoroNav designs text-based descriptions of paths and images that are readily interpretable by a large language model (LLM). Our approach presents a synergy of path and farsight descriptions to represent the environmental context, enabling the LLM to apply commonsense reasoning to ascertain the optimal waypoints for navigation. Extensive evaluation on the HM3D and HSSD datasets validates that VoroNav surpasses existing ZSON benchmarks in both success rates and exploration efficiency (+2.8% Success and +3.7% SPL on HM3D, +2.6% Success and +3.8% SPL on HSSD). Additionally introduced metrics that evaluate obstacle avoidance proficiency and perceptual efficiency further corroborate the enhancements achieved by our method in ZSON planning.

1. Introduction

Navigation capability holds great significance for household robots, enabling these machines to effectively reach designated areas and complete various subsequent tasks. Within this context, Zero-Shot Object Navigation (ZSON) demands that an agent have the ability to move toward a target object of an unfamiliar category by leveraging scene reasoning, a capability essential for the performance of diverse complex tasks by household robots. The core of ZSON centers on making good use of general commonsense to steer agents for accurate localization of a novel target object and exploration with minimal movement cost.

*Equal Contribution

†Corresponding Authors



Figure 1. **Voronoi-based Navigation with LLM.** Our model focuses on optimizing the decision-making process in ZSON. It enables the agent to pinpoint intersections rich in observation on the map by Voronoi sparsification, which act as navigational waypoints. The agent perceives the environment at intersections, collects scene information from nearby waypoints, and performs reasoning guided by LLM to ascertain the most plausible waypoint leading to the desired target. The five images presented in (a) depict the agent’s corresponding perspectives as it faces five adjacent navigational waypoints at the intersection illustrated in (b). The numbers in (a) show the correspondence with waypoints in (b).

Current ZSON methods can be categorized into two types: end-to-end network-based navigation [5, 21, 24, 35]

and map-based navigation [6, 7, 36]. The output provided by the end-to-end model lacks interpretability and necessitates a substantial amount of training data. This leads to a significant gap between the model’s output actions and those derived from map-based methods, particularly in terms of coherence and long-term planning capabilities. Regarding actual performance, the end-to-end methods exhibit inefficiency problems of back-and-forth redundant movement. In contrast, map-based navigation methods usually plan new waypoints either every predetermined number of steps or when the increment in map building reaches a specific threshold. However, the decision points selected by the map-based approaches come short of optimal positions for decision-making because the agent could potentially uncover expansive unseen areas by just one more step from here, which can bring huge benefits to scene reasoning and task planning. Just imagine, if you are looking for an object, walking down a long corridor, and encountering the scene shown in Fig. 1, would you be more inclined to halt at the intersection, take a moment to observe your surroundings, and then make a thoughtful decision after comparing the adjacent areas?

Another significant issue faced by existing navigation algorithms is the integral representation of observed scenes for subsequent planning. When presented with RGB images, network-based approaches leverage semantic embeddings to identify object categories and utilize recurrent policy networks to directly predict optimal actions; Conversely, map-based methods mostly employ an open-set detector to segment RGB images, which, in conjunction with depth and position information, are utilized to construct a semantic map. By interpreting the representation of the semantic map, the next subgoal point is selected. Each method, however, presents distinct limitations: network-based methods struggle with low exploration efficiency and constrained planning memory that is limited by implicit scene representation and network size, whereas map-based methods only build maps within the field of view of the depth camera, thus unable to integrate information beyond the sensing range of depth images to plan informed waypoints.

To address these challenges, our paper focuses on the following aspects: (1) designing a zero-shot strategy to predict informative waypoints for decision-making; (2) adopting text-based scene descriptions to represent the surrounding environment, integrating the information of both semantic map and images; (3) leveraging commonsense reasoning to decide on waypoints.

In particular, we propose a **Voronoi-based zero-shot object Navigation (VoroNav)** framework to improve the planning process of map-based navigation. During navigation, a real-time semantic map is maintained to represent the coarse-grained depiction of the surrounding environment. This study put insight into the positive impact of

making decisions at intersections in the field of navigation, demonstrating how decision locations affect navigation effectiveness. Consequently, we develop a Reduced Voronoi Graph (RVG) generation approach to distill intersection points and viable pathways from the dynamically updated semantic map. Utilizing the graph-structured scene representation, we systematize the planning process by breaking it down into a sequence of point-to-point navigation sub-tasks across the graph nodes. Specifically, we construct a two-dimensional representation of semantic information: path descriptions and farsight descriptions. Path descriptions fully exploit the edge information generated by RVG to record the sequence of scenarios encountered along the pathway to the unexplored area. Farsight descriptions can depict the panoramic scenes at intersections, which can absorb semantic information beyond the scope of the map. Considering the training-free nature of ZSON, we propose a systematic prompt generation mechanism and utilize the large language model GPT-3.5 [23] to carry out commonsense reasoning and decision-making tasks. In fact, the prompt is generated by integrating both path descriptions and farsight descriptions to form the fused scene text descriptions, with which GPT-3.5 then predicts the semantic rewards of neighboring intersections as crucial clues for exploration. The agent selects the most suitable navigation waypoint that maximizes the navigation rewards, which take into account environmental exploration, path efficiency, and commonsense tendencies.

Our contributions can be summarized as follows:

- We introduce Voronoi-based scene graph generation for ZSON, designed to select waypoints that provide a wealth of observation data to facilitate subsequent planning processes.
- We design an innovative fusion strategy for scene representation that combines both path and farsight descriptions to provide more holistic information for LLM to analyze and evaluate, avoiding the limitation associated with the narrow field-of-view inherent in map-based methodologies.
- We achieve state-of-the-art results on the ZSON task and outperform benchmark methods on representative datasets, i.e., HM3D [26] and HSSD [12].

2. Related Work

2.1. Zero-shot Object Navigation

In contrast to conventional object navigation, zero-shot object navigation aims to enhance its capacity to locate objects of unfamiliar categories and attain better efficiency in exploration. Image-based ZSON works [1, 7, 21] map the egocentric images and target object instructions to the embedding spaces, utilizing a trained policy network to predict subsequent actions. Map-based ZSON works mostly adopt

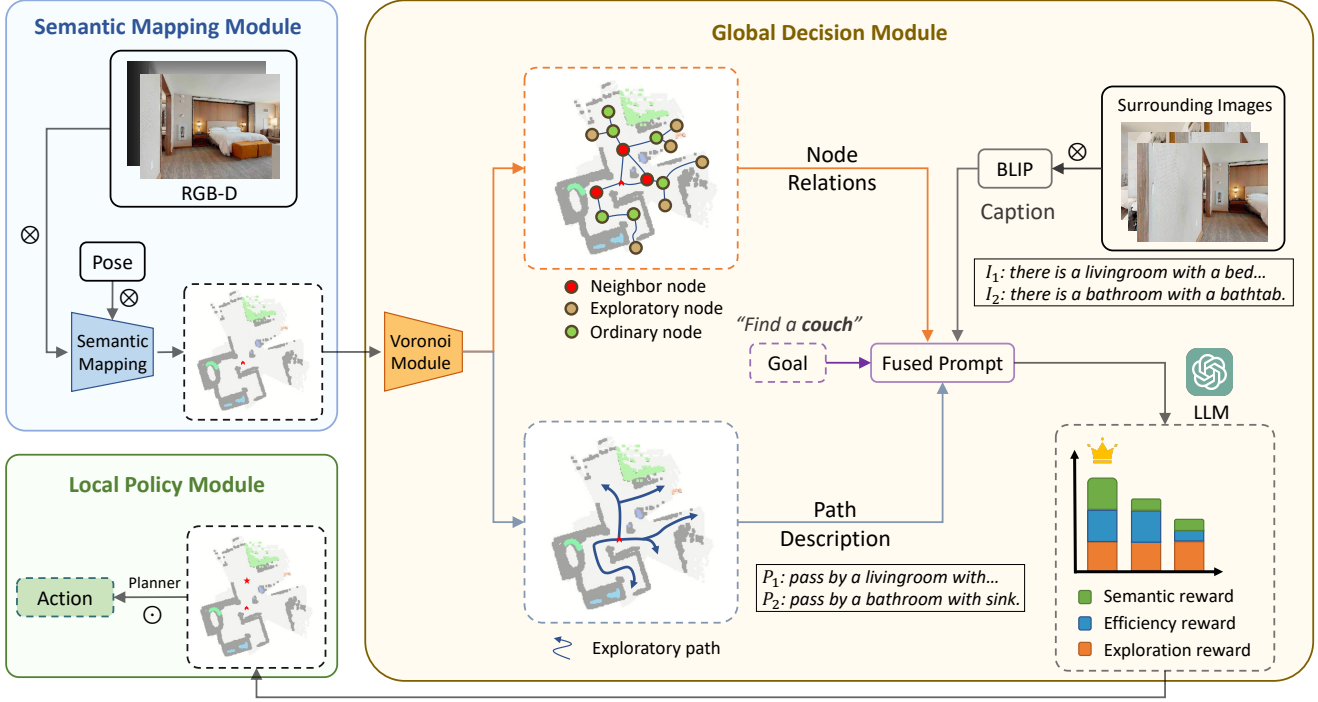


Figure 2. **VoroNav** includes three modules. All perceptual inputs are marked with \otimes , and the output of the agent is “Action” (marked with \odot). The RGB-D and pose observation are processed by the Semantic Mapping Module (light blue module) to form a semantic map. The Global Decision Module (light yellow module) generates RVG, which is used to produce the textual descriptions of surrounding neighbor nodes and exploratory paths. It then employs an LLM to assist in selecting the promising neighbor node as a mid-term goal by inferring the fused prompt of scene descriptions. The Local Policy Module (light green module) plans the low-level actions of the agent to reach the target point.

hierarchical structures, integrated with zero-shot object detectors that identify target objects. These approaches make informed decisions by leveraging prior knowledge of object relationships [6] or by employing large language models [29, 34, 36].

2.2. Scene Representation for Navigation

In the hierarchical framework of visual navigation, scene representation is used to process the received observation information into an explicit structure that can be directly utilized by subsequent decision-making. Frontier-based works [6–8, 27] model semantic information into frontiers extracted by online grid maps to complete exploration with specific tasks. Graph-based works predict waypoints directly from RGB-D images [2, 14, 15] or from sparsified maps [16, 18, 19] to represent the environment as topological maps, integrating geographic and semantic information into nodes for waypoint navigation. [10] proposes a large-size model that can read the 3D scenes, extract the features from the 3D point cloud generated by the entire scene, and provide targeted planning solutions for diverse tasks.

2.3. LLM Guided Navigation

The large language model (LLM) has become a new way of prior-knowledge reasoning in navigation due to its powerful information processing and compatibility capabilities. [36] uses LLM to predict the degree of correlation with the target object at the object level and the room level. [34] generates clusters of unexplored areas by frontiers, and leverages LLM to infer the correlation between the target object and the objects contained within each cluster. [7] uses LLM to provide prior information at the object level to assist in target object localization. [29] feeds chain-of-thought (CoT) into LLM for navigation that encourages exploration of areas with higher relevance while concurrently avoiding moving to areas that are unrelated to the target object. [4] clusters panoramic images into scene nodes by LLM, uses CoT of LLM to determine whether exploration or exploitation, selects the image with the highest likelihood of finding the target object, and navigates accordingly based on the chosen image. [33] applies the decision-making of LLM in multi-robot collaborative navigation. By extracting information such as obstacles, frontiers, object coordinates, and robot states from online maps, the LLM centrally plans the mid-term goal for each robot.

3. VoroNav Approach

This section first introduces the task definition of ZSON (Section 3.1). An overview of the VoroNav framework is then provided (Section 3.2), followed by the details of VoroNav, including the creation of a semantic map (Section 3.3), the selection of mid-term goal points (Section 3.4), and the local motion planning (Section 3.5). Finally, the VoroNav procedure for executing a complete episode is summarized (Section 3.6).

3.1. Task Definition of ZSON

Traditional supervised object navigation relies on the knowledge or reward from the training data to predict the optimal action a_t and is limited to navigating to targets within a closed set of known categories \mathcal{K} . However, the ZSON task requires neither purposeful training nor closely linked prior knowledge for navigation toward a novel set of object types \mathcal{N} . Initially, the agent is placed at a designated start point p_0 and is given the category $G \in \mathcal{N}$ of the target to find. The agent’s observation includes RGB-D images I_t and the real-time pose p_t in the environment \mathcal{E} . An effective decision-making framework needs to be developed to leverage these observed data $\mathcal{O}_t = \{\{p_0, I_0\}, \dots, \{p_t, I_t\}\}$ to understand and deduce the environment, aiming to predict the likely position of the target object. The agent is required to explore the environment according to its planning module until it discovers the target, after which it should proceed toward the target. Success is achieved when the agent reaches a geodesic distance of less than 0.1 meters from the target and executes a “Stop” command. Conversely, the task is deemed failed if the agent either exceeds the maximum step count without finding the target or executes the “Stop” action at a distance greater than 0.1 meters from the target.

3.2. Method Overview

As shown in Fig. 2, our VoroNav framework comprises three modules: the Semantic Mapping Module, the Global Decision Module, and the Local Policy Module. The overall framework receives real-time RGB-D images and the agent’s pose as inputs, stores historical images simultaneously, and the outputs consist of discrete low-level actions such as turning and advancing.

The Semantic Mapping Module is tasked with constructing an incremental semantic map from the continuous stream of RGB-D images and pose data. The Global Decision Module first employs the Voronoi sparsification to delineate the map’s unoccupied space and construct a Voronoi graph. Subsequently, the agent generates the fused descriptions of the exploratory paths and neighbor nodes that are derived from the Voronoi graph. It then employs a large language model to interpret the fused descriptions, effectively merging exploration, efficiency, and semantic considerations to determine the most suitable mid-term goal. Once

the goal point is given, the Local Policy Module computes the shortest path from the current location to the goal on the constructed map and selects a discrete action according to the planned path.

3.3. The Semantic Mapping Module

We maintain a 2D semantic map \mathcal{M}_t by processing RGB-D images $\{I_0, \dots, I_t\}$ and poses $\{p_0, \dots, p_t\}$. This semantic map is structured as a $(K + 2) \times M \times M$ grid, where M denotes the dimensions of the map’s width and height, and $(K + 2)$ indicates the total number of channels within the map. These channels comprise K categorical maps, an obstacle map, and an explored map, which correspond to detected object regions, obstacle regions, and observed regions, respectively. Given the depth image and the agent’s pose, 3D point clouds are generated. All point clouds near the floor are assigned to the explored map representing the feasible area to travel through, whereas those at other heights are mapped into the obstacle map. Meanwhile, we predict the category masks of the RGB image by Grounded-SAM [13, 20] and map the masks into 3D semantic point clouds using the depth information and the agent’s pose. The 3D point clouds associated with categorical information are mapped onto K distinct categorical channels.

3.4. The Global Decision Module

Graph Extraction. The Generalized Voronoi Diagram (GVD) of a map depicts a set of points that are equidistant from the two closest obstacle points, representing the medial-axis pathway of unoccupied space outside the obstacles of arbitrary shape. Let $\mathcal{X} \in \mathbb{R}^2$ be the map space and Ω denote the area occupied by obstacles on the map. The point set \mathcal{V} of GVD can be represented as follows:

$$\mathcal{V} = \{x \in \mathcal{X} \setminus \Omega \mid \exists \omega_i \neq \omega_j, d(x, \omega_i) = d(x, \omega_j) = f(x)\} \quad (1)$$

where $\omega_{(\cdot)}$ represents any point within the obstacles Ω , the function $d(\cdot, \cdot)$ denotes the Euclidean distance between two points, while $f(\cdot)$ signifies the positive *Euclidean Signed Distance Field* (ESDF), which is defined as follows:

$$f(x) = \inf_{y \in \partial\Omega} d(x, y) \quad (2)$$

where $\partial\Omega$ indicates the boundary of the obstacles.

Given the obstacle and explored maps, we can obtain the unoccupied map by logically subtracting the obstacle map from the explored map, representing the traversable areas within the observed regions. We then preprocess the unoccupied map by using the morphology methods [30] to fill holes and smooth boundaries. To obtain the GVD, we extract a set of Voronoi points \mathcal{V} by skeletonizing the unoccupied map (Figure 3 (a)). Subsequently, to manifest the connectivity and accessibility of the unoccupied map, the GVD can be processed into RVG \mathcal{G} , a graph form with

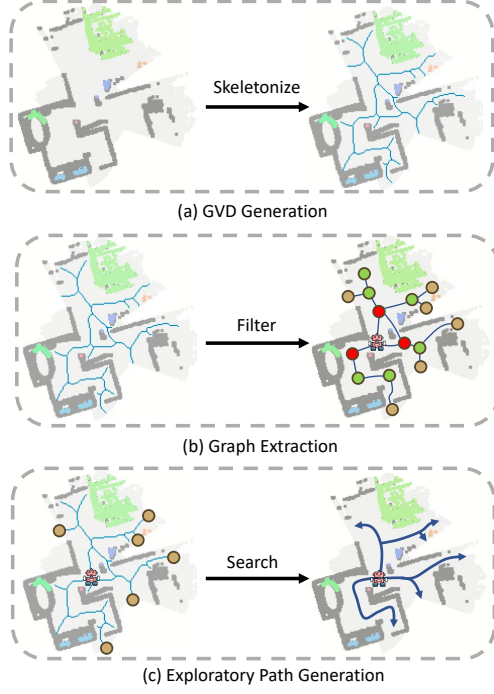


Figure 3. **The Voronoi Processing Module.** In (a), we skeletonize the areas that are not occupied by obstacles in the explored area and obtain the GVD (blue lines). In (b), the nodes and edges are extracted in GVD to form the RVG. The agent nodes (robot icon), neighbor nodes (red circles), ordinary nodes (green circles), and exploratory nodes (orange circles) are filtered by the location of the nodes. In (c), the exploratory paths (blue arrows) are generated by searching for the shortest paths on the GVD from the agent node to the exploratory nodes.

nodes V and edges E (Figure 3 (b)). The nodes correspond to GVD points that are either at intersections or on the endpoint of GVD, while the segments directly connecting two adjacent nodes are identified as edges. The raw graph is then preprocessed through operations such as merging proximate nodes and eliminating trivial forks. We classify the RVG nodes into four categories based on the node positions: *agent nodes*, *neighbor nodes*, *exploratory nodes*, and *ordinary nodes*. Specifically, the node closest to the agent is designated as the agent node, representing the agent’s current decision-making position; The nodes directly connected to the agent node are considered neighbor nodes for subsequent planning; The nodes adjacent to unexplored areas with a single connecting edge are classified as exploratory nodes. All the other nodes are categorized as ordinary nodes.

Path Description. We generate navigable paths formed by RVG edges and create text descriptions that embody the scene along each path, as shown in Figure 4 (a). To be specific, given m exploratory nodes, we leverage the Wavefront Propagation method [11] to obtain the short-

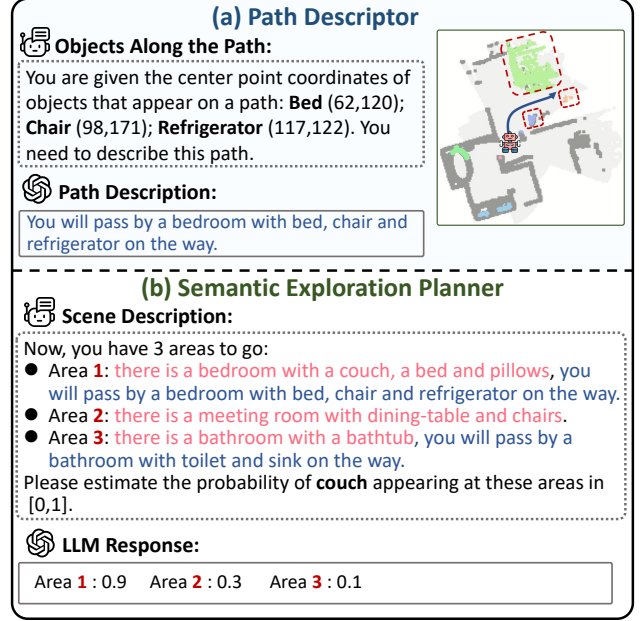


Figure 4. **Commonsense Reasoning of LLM.** In (a), LLM analyzes the objects and coordinates that appear on the path and depicts the scene along the path. In (b), LLM predicts the probability of the target object appearing in each area by comprehending the fused text descriptions.

est path P_j from the agent node to the j^{th} exploratory node on the GVD and compile all the paths into a set $\mathcal{P} = \{P_1, \dots, P_m\}$, as shown in Figure 3 (c). To generate the semantic description of each path P_j , we gather from the semantic map the occurrence of c objects $\{o_{j,1}, \dots, o_{j,c}\}$ along the exploratory path P_j and the objects’ central locations $\{l_{j,1}, \dots, l_{j,c}\}$. Assuming paths within the set $\{P_a, \dots, P_b\}$ all pass through the neighbor node N_i , prompts of the form $\text{Template}(\{P_a : (o_{a,1}, l_{a,1}), \dots\} \cup \dots \cup \{P_b : (o_{b,1}, l_{b,1}), \dots\})$ are generated for the neighbor node N_i , by collecting and summarizing the semantic information along the paths in $\{P_a, \dots, P_b\}$. The function $\text{Template}(\cdot)$ processes the input data, converting it into the textual form and integrating it with predefined templates to create a format conducive to conversational interactions with LLM (refer to Figure 4 (a): *Objects Along the Path*). Afterward, to distill the fragmented and unstructured path information into a coherent format, we employ GPT-3.5, which possesses robust comprehension and generative capabilities, for creating the scene descriptions D_i^p along paths that traverse each neighbor node N_i (refer to Figure 4 (a): *Path Description*). Similarly, assuming there involves n neighbor nodes, we describe the scenes of the paths each neighbor node N_i leads to and compile the path descriptions into a set $\mathcal{D}^p = \{D_1^p, \dots, D_n^p\}$. This process textualizes the scenarios the agent will encounter along possible navigable paths after reaching each neighbor node.

Farsight Description. Path description generation is the process of converting the semantic map into scene descriptions of path form; however, the semantic map is constrained by the depth camera’s limited range, precluding the incorporation of map information beyond its scope. Consequently, semantic descriptions of RGB images of unexplored areas adds crucial complementary context for robot navigation. As shown in Fig. 5, at the onset of the ZSON task or upon reaching an RVG node, the agent executes a full rotation to capture panoramic images. We then determine the ray R_i on the map that extends from the agent’s current node (agent node) to each neighbor node N_i . The RGB image I_k collected from the full rotation $\mathcal{I}_t = \{I_{t-11}, \dots, I_t\}$ (a full rotation includes 12 turns), whose central *Line of Sight* (LoS) T_k exhibits the least angular deviation from the ray R_i , is identified as the one (I_i^f) oriented towards the corresponding neighbor node N_i . Let $\mathcal{T}_t = \{T_{t-11}, \dots, T_t\}$ be the central LoS set of \mathcal{I}_t , the process of matching images with each neighbor node N_i can be defined as follows:

$$\begin{aligned} \arg \min_{T_k} \quad & g(R_i, T_k) \\ \text{s.t.} \quad & T_k \in \mathcal{T}_t \end{aligned} \quad (3)$$

where the function $g(\cdot, \cdot)$ indicates the angle between two rays on the map. The BLIP model [17] is then employed to generate descriptions $\mathcal{D}^f = \{D_1^f, \dots, D_n^f\}$ for those images $\{I_1^f, \dots, I_n^f\}$ facing different neighbor nodes $\{N_1, \dots, N_n\}$.

Planning with LLM. We select the mid-term target points by considering three distinct factors: exploration objective, locomotion efficiency (traversed path length), and alignment with typical scene layouts. The rewards for exploration and efficiency are space reasoning results stemming from spatial topology. Conversely, semantic rewards are reasoning feedback grounded in empirical knowledge and commonsense.

To encourage the agent to explore the environment, we design a binary exploration reward vector \mathbf{P} with the highest priority compared to other aspects. This involves assessing whether each neighbor node facilitates access to previously unexplored regions. Specifically, we evaluate if there exists an exploratory path from the agent node to each exploratory node that traverses through neighbor nodes, thereby ascertaining the exploratory significance of these neighbor nodes.

Considering exploration efficiency, the Frontier-based methods face challenges in precluding the agent’s redundant traversal across previously explored areas, a phenomenon that can lead to significant distance loss. To mitigate this issue, we have designed an efficiency reward vector \mathbf{C} and integrated a strategy that promotes the exploration of novel paths into our graph-based framework. The decision-making process entails assessing whether each neighbor

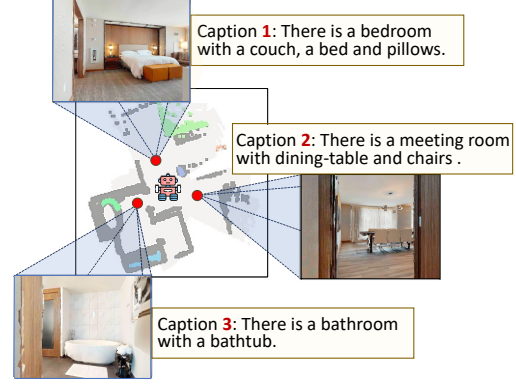


Figure 5. **Farsight Image Captioning.** The agent selects all RGB images that capture the views of neighbor nodes and uses BLIP to generate captions of these images.

node lies within the previously traversed area. Nodes not on the historical trajectories are deemed efficient targets for further exploration.

The Global Decision Module utilizes the commonsense reasoning capabilities of the large language model, GPT-3.5, to select the most promising goal node for finding or approaching the target object among all neighbor nodes. To this end, we combine the path and farsight descriptions of each neighbor node to generate a specially designed form of prompt that is amenable for GPT-3.5. This enables the LLM to more accurately estimate the probability of the target object’s presence on each neighbor node by detailed prompts, as illustrated in Fig. 4 (b). The probabilities given by the LLM’s response are compiled into a semantic reward vector \mathbf{L} and serve as varying levels of semantic incentive to navigate towards neighbor nodes.

When the agent simultaneously considers exploration, efficiency, and semantic aspects of decision-making, balancing the priority among these factors becomes challenging. To mitigate potential conflicts, we have implemented a hierarchical structure within the reward system. Assuming there are a total of n neighbor nodes, the cumulative reward vector $\mathbf{W} \in \mathbb{R}^n$ is the sum of exploration reward vector \mathbf{P} , efficiency reward vector \mathbf{C} and semantic reward vector \mathbf{L} . The next navigation point selection can be formulated as follows:

$$\begin{aligned} \arg \max_{\mathbf{S}} \quad & \mathbf{W}^T \mathbf{S} \\ \text{s.t.} \quad & \mathbf{S} \in \mathbb{E}^n \end{aligned} \quad (4)$$

where $\mathbb{E}^n = \{\mathbf{e}_1, \mathbf{e}_2, \dots, \mathbf{e}_n\}$, which is the standard orthogonal basis composed of n -dimensional coordinate vectors, the decision variable $\mathbf{S} = \mathbf{e}_i$ if i^{th} neighbor node is selected for next navigation waypoint, the reward vectors

are defined as follows:

$$\begin{cases} \mathbf{W} = \mathbf{P} + \mathbf{C} + \mathbf{L}, \\ \mathbf{P} = 2(\alpha_1 \mathbf{e}_1 + \dots + \alpha_n \mathbf{e}_n), \\ \mathbf{C} = \beta_1 \mathbf{e}_1 + \dots + \beta_n \mathbf{e}_n, \\ \mathbf{0} \leq \mathbf{L} \leq \mathbf{1}, \\ \alpha_i, \beta_i \in \{0, 1\}, \\ \mathbf{W}, \mathbf{P}, \mathbf{C}, \mathbf{L} \in \mathbb{R}^n. \end{cases} \quad (5)$$

where the i^{th} dimensional component of \mathbf{L} is the semantic score of the i^{th} neighbor node provided by LLM within the interval $(0, 1)$. The binary coefficient $\alpha_i \in \{0, 1\}$ stands for whether the i^{th} neighbor node is traversed through by exploratory paths ($\alpha_i = 1$) or not ($\alpha_i = 0$), and $\beta_i \in \{0, 1\}$ denotes whether the i^{th} neighbor node is covered by historical trajectories ($\beta_i = 0$) or not ($\beta_i = 1$). We establish the hierarchy of priorities for each aspect by assigning different reward weights of the reward vectors as shown in Equation (5) (1st : Exploration; 2nd : Efficiency; 3rd : Semantic).

To illustrate the robustness of VoroNav in various challenging scenarios and the roles played by distinct reward vectors, we have visualized a worst-case navigation example and the details of cumulative rewards, as shown in Figure 6. For exploration purposes, only neighbor nodes traversed along the exploratory path indicate its heading toward unexplored areas, which is foremost for the exploration process (refer to Figure 6 (c)); Concerning efficiency, we rely on the agent’s historical decisions, considering the current agent node as the optimal choice from previous decisions and discouraging turning back. If there is one or more extensions from the agent node leading to unexplored areas, the agent is inclined to continue its ongoing exploration (refer to Figure 6 (a)). Conversely, if no extension offers exploratory paths, it indicates that unexplored regions exist elsewhere, and historically traversed nodes will be revisited, prompting the agent to return to previously traveled paths (refer to Figure 6 (b)). Thus, the agent prioritizes exploration and efficiency from topological perspectives in the navigation. In cases where multiple nodes hold equivalent exploration and efficiency rewards, the agent will proceed to the neighbor node where the target object is more likely to be found, as indicated by the higher predicted semantic probability (refer to Figure 6 (a)).

We select the neighbor node that offers the highest cumulative reward as the next target waypoint for navigation. If the agent’s vision model identifies the target object G while exploring, the Semantic Mapping module will map the target’s point cloud onto the existing map \mathcal{M} , enabling direct path planning toward the target’s location.

3.5. The Local Policy Module

Given the agent’s pose, obstacle map, and target point, we use the Fast Marching Method [28] to find the shortest path from the current position to the target, which is com-

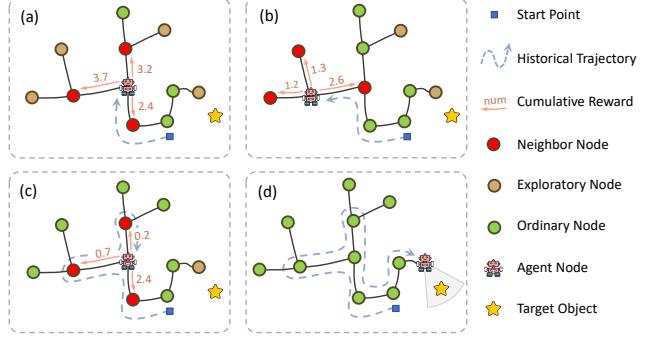


Figure 6. **A Worst-case Example.** This figure depicts the exploration process on RVG and the cumulative rewards of neighbor nodes when LLM alone makes undesirable decisions. (a) Three neighbor nodes are traversed by exploratory paths, one of which has been passed by the agent, and the agent compares LLM scores between the other two to make a choice. (b) Two nodes have not been passed by the agent but are not traversed by exploratory paths, and another node that the agent has passed by but with an exploratory path traversed is selected as a mid-term goal. (c) Three neighbor nodes have all been passed by the agent, but one of them leads to an unexplored area and is selected as a mid-term goal. (d) The agent finds the target object after exploration.

posed of a sequence of discrete points in the map. The nearest coordinate on this shortest path is selected as an immediate navigation objective for executing actions such as moving forward or turning. Once arriving at a Voronoi node, the agent will rotate and repeat the selection of the mid-term goal.

3.6. Navigation Process

A complete process of a navigation episode is illustrated in Algorithm 1. The code snippet of the *LookAround* procedure, as presented in Algorithm 1, is further elaborated in Algorithm 2. At the beginning of each episode, the subgoal is initially empty. At each step, the agent updates the semantic map of its surroundings and the RVG accordingly (Line 2-6). If the agent detects the target object at any time, it will immediately plan a direct route to approach the object (Line 7-8). Conversely, if the target remains undetected, the agent performs a complete rotation to establish a preliminary RVG scene representation (Line 11, Algorithm 2). The agent then navigates to the closest RVG node (Line 12). Upon reaching the RVG node or the mid-term goal (Line 13), the agent rotates a full circle again (Line 14, Algorithm 2), derives the exploratory paths (Line 15) and surrounding images (Line 16), generates corresponding descriptions of paths (Line 17-18) and farsight (Line 19) integrated with the respective neighbor nodes. A large language model is then employed to evaluate the fused descriptions of each neighbor node, obtaining semantic rewards based on the results of scene reasoning (Line 20). Concurrently,

Algorithm 1: Navigation Process of VoroNav

Input: Target object G
Initialize: Initial observation $\mathcal{O}_0 \leftarrow \emptyset$
Initial semantic map $\mathcal{M}_0 \leftarrow \emptyset$
Step Number $t \leftarrow 1$
 $SubGoal \leftarrow None$

```
1 while Episode is not done do
2    $\mathcal{O}_t \leftarrow \mathcal{O}_{t-1} \cup \{p_t, I_t\}$ 
3    $ObjectMasks \leftarrow \text{GroundedSAM}(I_t)$ 
4    $\mathcal{M}_t \leftarrow \text{Mapping}(\mathcal{M}_{t-1}, \mathcal{O}_t, ObjectMasks)$ 
5    $\mathcal{V} \leftarrow \text{Skeletonize}(\mathcal{M}_t)$ 
6    $\mathcal{G} \leftarrow (V, E) \leftarrow \text{Filter}(\mathcal{M}_t, \mathcal{V})$ 
7   if  $G$  exists in  $\mathcal{M}_t$  then
8      $SubGoal \leftarrow \text{Location}(\mathcal{M}_t, G)$ 
9   else
10    if  $SubGoal$  is None then
11      LookAround;
12       $SubGoal \leftarrow \text{Nearest}(p_t, V)$ 
13    if Agent reaches node in  $V$  then
14      LookAround;
15       $\mathcal{P} \leftarrow \text{Search}(p_t, \mathcal{G})$ 
16       $NeighborImages \leftarrow \text{Select}(\mathcal{I}_t, \mathcal{M}_t, V)$ 
17       $PathPrompt \leftarrow \text{Template}(\mathcal{M}_t, \mathcal{G}, \mathcal{P})$ 
18       $\mathcal{D}^p \leftarrow \text{LLM}(PathPrompt)$ 
19       $\mathcal{D}^f \leftarrow \text{BLIP}(NeighborImages)$ 
20       $\mathbf{L} \leftarrow \text{LLM}(G, \mathcal{D}^p, \mathcal{D}^f)$ 
21       $\mathbf{P} \leftarrow \text{Exploration}(V, E)$ 
22       $\mathbf{C} \leftarrow \text{Efficiency}(\mathcal{M}_t, \mathcal{O}_t, V)$ 
23       $SubGoal \leftarrow \text{Decision}(V, \mathbf{P}, \mathbf{C}, \mathbf{L})$ 
24    $a_t \leftarrow \text{FMM}(\mathcal{M}_t, p_t, SubGoal)$ 
25    $t \leftarrow t + 1$ 
```

Result: Episode ends.

the agent acquires exploration rewards (Line 21) and efficiency rewards (Line 22) on the neighbor nodes by analyzing the layout of unexplored areas and historical trajectories. The neighbor node with the highest cumulative reward will be selected as the optimal mid-term goal point for exploration (Line 23). Finally, low-level motion planning is utilized to devise a sequence of actions targeting the mid-term goal (Line 24). If the agent reaches the vicinity of the identified target or takes actions surpassing the maximum number of steps, it will immediately issue a “Stop” action and the episode ends.

4. Experiments

In order to assess the navigation capability and exploration efficiency of VoroNav, we conducted extensive experiments on the two representative datasets: the HM3D and HSSD datasets.

Algorithm 2: LookAround

```
1  $\mathcal{I}_{t+12} \leftarrow \emptyset$ 
2 for  $i \leftarrow 1$  to 12 do
3    $a_t \leftarrow \text{TurnRight}$ 
4    $t \leftarrow t + 1$ 
5    $\mathcal{O}_t \leftarrow \mathcal{O}_{t-1} \cup \{p_t, I_t\}$ 
6    $ObjectMasks \leftarrow \text{GroundedSAM}(I_t)$ 
7    $\mathcal{M}_t \leftarrow \text{Mapping}(\mathcal{M}_{t-1}, \mathcal{O}_t, ObjectMasks)$ 
8    $\mathcal{V} \leftarrow \text{Skeletonize}(\mathcal{M}_t)$ 
9    $\mathcal{G} \leftarrow (V, E) \leftarrow \text{Filter}(\mathcal{M}_t, \mathcal{V})$ 
10   $\mathcal{I}_{t+12-i} \leftarrow \mathcal{I}_{t+12-i} \cup \{I_t\}$ 
11 if  $G$  exists in  $\mathcal{M}_t$  then
12    $SubGoal \leftarrow \text{Location}(\mathcal{M}_t, G)$ 
13 continue
```

4.1. Baselines and Metrics

Datasets. The HM3D dataset provides 20 high-fidelity reconstructions of entire buildings and contains 2K validation episodes for object navigation tasks. The HSSD dataset provides 40 high-quality synthetic scenes and contains 1.2K validation episodes for object navigation.

Evaluation Metrics. We adopt Success rate (Success) and Success weighted by Path Length (SPL) as the evaluation metrics [3], which are defined as follows:

- **Success** represents the percentage of successful episodes to the total number of episodes.
- **SPL** quantifies the agent’s mobility efficiency in goal-oriented navigation by calculating the inverse ratio of the actual path length traversed to the optimal path length weighted by success rate. This metric indicates the degree of conformity between the predicted actions and the oracle decisions.

Baselines. We conduct comparative evaluations of VoroNav and representative baseline planners, including:

- **Random Exploration** drives the robot to march to randomly sampled points in unexplored areas.
- **Frontier** [32] is an exploration method that selects the nearest boundary points of unexplored areas and unoccupied areas as the mid-term goals.
- **Voronoi** corresponds to VoroNav but without considering the semantic reward.
- **L3MVN** [34] is a region-oriented navigation method that leverages LLM to select mid-term waypoint by evaluating regions clustered by the frontier points.
- **Pixel-Nav** [4] is an image-based navigation method that analyzes panoramic images and utilizes LLM to determine the optimal pixel for exploration.
- **ESC** [36] is a pioneering method employing an LLM to determine the mid-term goal from the frontier points during exploration.

Planner	Method	Training-free	LLM	HM3D		HSSD	
				Success \uparrow	SPL \uparrow	Success \uparrow	SPL \uparrow
Random	Random Exploration*	Yes	-	26.5	9.2	30.2	12.7
Topological	Frontier [32]*	Yes	-	33.7	15.3	36.0	17.7
	Voronoi*	Yes	-	38.7	23.3	40.3	22.2
Semantic	L3MVN [34]*	Yes	GPT-2-Large [25]	35.2	16.5	38.4	19.4
	Pixel-Nav [4]	No	GPT-4 [22]	37.9	20.5	-	-
	ESC [36]	Yes	GPT-3.5 [23]	39.2	22.3	-	-
	VoroNav(Ours)	Yes	GPT-3.5-turbo [23]	42.0	26.0	41.0	23.2

Table 1. **Comprison with ZSON Baselines.** Our proposed VoroNav outperforms the ZSON baselines on both HM3D and HSSD. To guarantee the zero-shot navigation capability of each method, we use Grounded-SAM to replace the vision modules of methods marked by an asteroid (*), which aligns with our model.

Note that Random Exploration, Frontier, and Voronoi methods only utilize topological information of the map for planning, while L3MVN, Pixel-Nav, and ESC additionally require semantic information.

4.2. Experiment Setup

Evaluations on HM3D follow settings outlined in the Habitat ObjectNav challenge 2022 [31]. Evaluations on HSSD adopt the same validation parameters utilized in [12]. In both datasets, the agent is a LoCoBot [9] with a base radius of 0.18m, outfitted with an RGB-D camera mounted at a height of 0.88 meters and a pose sensor that provides accurate localization. The camera has a 79° *Horizontal Field of View* (HFOV) and frame dimensions of 480×640 pixels. The agent’s action space is {Stop, MoveForward, TurnLeft, TurnRight, LookUp, LookDown}, with a discrete movement increment of 0.25m and discrete rotations of 30°. The object goal categories in episodes include “bed”, “chair”, “sofa”, “tv”, “plant”, and “toilet”.

4.3. Results and Analysis

4.3.1 Comparison with SOTA Methods

As shown in Table 1, our approach outperforms the best-performing competitor (+2.8% Success and +3.7% SPL on HM3D, +2.6% Success and +3.8% SPL on HSSD). As expected, the Random Exploration method suffers from the blind exploration strategy, resulting in a high likelihood of targeting the wrong areas and walking back and forth during exploration. The Frontier method consistently pursues the closest unexplored boundary, resulting in a more rapid exploration compared to the Random Exploration. Yet, the Frontier method suffers from relatively low efficiency as it fails to prioritize rapidly locating the target at the perception level. The Voronoi method shares similarities with the Frontier method in search for the nearest unexplored point. However, Voronoi enhances the naviga-

tion process by proceeding to informative neighbor nodes along the RVG paths, thereby pursuing to uncover larger areas with very few steps. Both L3MVN and ESC adopt the frontier exploration strategy and leverage an LLM to select appropriate frontier points, whereas Pixel-Nav makes decisions after a fixed number of steps, utilizing LLMs to predict the direction with the highest probability of leading to the target, and subsequently employing an RGB-based policy to plan a route and navigate accordingly. These three semantic planning methods uniformly make decisions at pre-determined intervals, which can lead to agents determining the mid-term goal in suboptimal positions with insufficient observations, thereby failing to fully unleash the reasoning power of LLM. Our VoroNav method further improves the navigation process while using scene descriptions of broader observations to assist LLM in decision-making, thereby achieving better performance. Figure 7 illustrates a successful episode of VoroNav navigating to the target with the help of the RVG and LLM.

4.3.2 Ablation Study

To manifest the contribution of each module, we compare VoroNav with three ablation models on both HM3D and HSSD datasets. The Voronoi method keeps the same settings as in Section 4.1. The Voro-path method omits the farsight descriptions in VoroNav and depends entirely on the path descriptions, whereas the Voro-image method excludes the path descriptions in VoroNav and depends merely on the farsight descriptions for decision-making. As indicated in Table 2, both Voro-path and Voro-image show higher Success and SPL than Voronoi, indicating the benefits of integrating semantic information to augment navigation capabilities. Furthermore, VoroNav exhibits superior performance compared to all ablation models, demonstrating the positive outcomes of integrating path and farsight descriptions to augment the reasoning capabilities of LLM.



Figure 7. **Simulation Experiments.** Utilizing LLM, the agent explores efficiently, discovers the target with a minimal path cost, and finally navigates to the target object with success. In this figure, we visualize the RGB images and semantic maps of the four global decision instances, and the dialog box on the left exhibits the conversation between the agent and LLM in the first global decision process.

Method	HM3D		HSSD	
	Success \uparrow	SPL \uparrow	Success \uparrow	SPL \uparrow
Voronoi	38.7	23.3	40.3	22.2
Voro-path	40.0	24.2	40.6	23.0
Voro-farsight	41.2	25.2	40.8	22.7
VoroNav	42.0	26.0	41.0	23.2

Table 2. **Ablation Study.** We compare VoroNav with three ablation models: (a). Voronoi: Voronoi-based navigation without any semantic guidance; (b). Voro-path: VoroNav that eliminates the farsight descriptions; (c). Voro-farsight: VoroNav that eliminates the path descriptions.

Method	HM3D		HSSD	
	Success \uparrow	SPL \uparrow	Success \uparrow	SPL \uparrow
Frontier	63.5	33.0	51.2	20.6
Voronoi	67.3	37.4	57.2	32.7
L3MVN	65.5	36.5	58.0	28.0
VoroNav	67.6	40.5	59.7	34.1

Table 3. **Ground-truth Semantics.** We find that after replacing the Grounded-SAM with ground truth semantic segmentation, our VoroNav still achieves the best performance, revealing the superiority of our planning module.

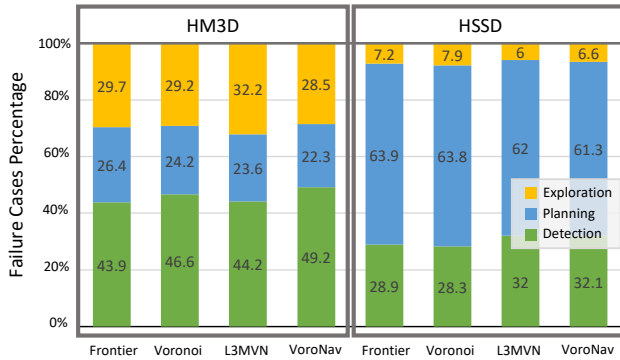


Figure 8. **Failure Cases Percentage.** In the failure statistics on HM3D and HSSD datasets, our VoroNav experiences fewest planning failures.

4.3.3 Failure Case Study

We have collected the reasons and frequencies of failures across all episodes, categorizing them into detection fail-

ures, planning failures, and exploration failures. Detection failure occurs when the agent mistakenly identifies non-target items as targets or overlooks the actual targets within the agent’s field of view. Planning failure arises when the agent gets stuck or fails to navigate to the target location despite having accurately detected the target. Exploration failure is attributed to the situation where the agent has not encountered the target within the assigned maximum number of steps.

As shown in Figure 8, we find that most failures are caused by incorrect detection in HM3D and by abnormal planning in HSSD. To eliminate the impact of detection errors during navigation and analyze the planning and exploration effects of navigation methods, we uniformly replace the RGB images across all methods with ground-truth semantic images. As shown in Table 3, when semantic priors of reasoning and planning are absent, the Voronoi method exhibits considerably superior performance in terms of both Success and SPL compared to the Frontier method. This enhancement in performance proves that within the topological domain, the Voronoi planning approach is more suit-

Method	HM3D		HSSD	
	SCA \uparrow	SEA \uparrow	SCA \uparrow	SEA \uparrow
Frontier	24.2	17.4	35.5	16.5
Voronoi	29.4	17.9	40.2	18.6
L3MVN	27.5	17.7	37.6	16.6
VoroNav	39.8	20.9	40.9	19.3

Table 4. **Planning Study.** We analyze the planning capability of different methods by comparing their SCA and SEA. Our proposed VoroNav method achieves the highest SCA and SEA metrics, indicating advanced capability for obstacle avoidance and low-cost exploration strategy.

able for goal-oriented navigation than the Frontier exploration method. With the guidance of LLM, VoroNav outperforms L3MVN by a large margin, further demonstrating that VoroNav’s information processing and decision-making are more effective for robot navigation with lower step cost and a higher success rate compared to L3MVN.

4.3.4 Planning Study

To verify that Voronoi-based methods are more suitable for visual navigation compared to Frontier-based methods, we introduce two metrics to evaluate the planning effect of each method: the Success weighted by Collision Avoidance (SCA) and the Success weighted by Explored Area (SEA).

The metric SCA quantifies the proportion of non-collision steps to the total number of agent forward steps weighted by success rate, manifesting the tendency of obstacle avoidance in navigation, which is defined as follows:

$$SCA = \frac{1}{N} \sum_{i=1}^N S_i \left(1 - \eta \frac{C_i}{F_i} \right), \quad (6)$$

where N is the total number of validation episodes, the binary variable $S_i \in \{0, 1\}$ indicates whether the i^{th} episode is successful ($S_i = 1$) or not ($S_i = 0$). The discount factor η is predetermined and varies across datasets. We set $\eta = 0.1$ in HM3D and $\eta = 1$ in HSSD. The variables C_i and F_i represent the number of collisions and forward steps in the i^{th} episode, respectively.

The metric SEA measures the normalized ratio of the observed region to the path length weighted by success rate, denoting the efficiency of perceiving the surrounding environment, which is defined as follows:

$$SEA = \frac{1}{N} \sum_{i=1}^N S_i \left(\gamma \frac{\sqrt{A_i}}{L_i} \right), \quad (7)$$

where A_i and L_i signify the area of the explored region and path length in the i^{th} episode, respectively. The discount

factor γ is also predetermined, and we set $\gamma = 0.002$ in HM3D and $\gamma = 0.01$ in HSSD.

As demonstrated in Table 4, we find that the SCA and SEA of Voronoi-based methods (Voronoi and VoroNav) significantly surpass those of Frontier-based methods (Frontier and L3MVN). The higher SCA score suggests that, throughout the exploration process, the mid-term goals of the Voronoi-based methods are typically chosen at intersections within unoccupied regions, which are less likely to be in proximity to obstacles, thereby reducing the incidence of collisions compared to the frontier-based methods. Specifically, if the agent gets too close to obstacles during navigation, it is easy to encounter blind spots in perceiving the surrounding environment, which can lead to collisions with undetected obstacles that lie within these blind spots during subsequent movement. In contrast, our method involves less movement near obstacles during exploration, allowing for wider unobstructed views and thus more comprehensive observations, resulting in safer navigation. Similarly, a higher SEA score indicates that the Voronoi-based methods favor intersections rich in information, enabling broader areas to be observed with minimal movement. The enhanced perceptual range increases the probability of the agent discovering the target directly. Meanwhile, this strategy yields potentially more valuable scene hints generated by comprehensive perception to inform LLM’s decision-making, thus heightening the chances of locating the target object.

5. Conclusion

We have presented the VoroNav framework that explores a novel form of graph representation for navigation space and substantially enhances ZSON by using a structured graph-based exploration strategy. Our approach circumvents the limitations of traditional end-to-end and map-based methods, by generating informative waypoints and representing the environment with an innovative fusion of text information. The RVG generation module, together with the use of GPT-3.5 for decision-making, leads to more strategic navigation and efficient exploration. By making use of LLM and topologically structured scene graphs, VoroNav sets a new benchmark for ZSON and opens up new pathways for intelligent robotic systems to interact with environments in a more human-like and intuitive manner.

Future work will focus on expanding the capabilities of VoroNav to handle more complex tasks, integrating multi-modal sensor information, and improving the framework’s robustness and adaptability to dynamic environments.

References

- [1] Ziad Al-Halah, Santhosh Kumar Ramakrishnan, and Kristen Grauman. Zero experience required: Plug & play modular transfer learning for semantic visual navigation. In *Proceed-*

- ings of the *IEEE/CVF Conference on Computer Vision and Pattern Recognition*, pages 17031–17041, 2022. 2
- [2] Dong An, Hanqing Wang, Wenguan Wang, Zun Wang, Yan Huang, Keji He, and Liang Wang. Etpnav: Evolving topological planning for vision-language navigation in continuous environments. *arXiv preprint arXiv:2304.03047*, 2023. 3
- [3] Peter Anderson, Angel Chang, Devendra Singh Chaplot, Alexey Dosovitskiy, Saurabh Gupta, Vladlen Koltun, Jana Kosecka, Jitendra Malik, Roozbeh Mottaghi, Manolis Savva, et al. On evaluation of embodied navigation agents. *arXiv preprint arXiv:1807.06757*, 2018. 8
- [4] Wenzhe Cai, Siyuan Huang, Guangran Cheng, Yuxing Long, Peng Gao, Changyin Sun, and Hao Dong. Bridging zero-shot object navigation and foundation models through pixel-guided navigation skill. *arXiv preprint arXiv:2309.10309*, 2023. 3, 8, 9
- [5] Hongyi Chen, Ruinian Xu, Shuo Cheng, Patricio A. Vela, and Danfei Xu. Zero-shot object searching using large-scale object relationship prior, 2023. 1
- [6] Junting Chen, Guohao Li, Suryansh Kumar, Bernard Ghanem, and Fisher Yu. How to not train your dragon: Training-free embodied object goal navigation with semantic frontiers, 2023. 2, 3
- [7] Samir Yitzhak Gadre, Mitchell Wortsman, Gabriel Ilharco, Ludwig Schmidt, and Shuran Song. Cows on pasture: Baselines and benchmarks for language-driven zero-shot object navigation. In *Proceedings of the IEEE/CVF Conference on Computer Vision and Pattern Recognition*, pages 23171–23181, 2023. 2, 3
- [8] Theophile Gervet, Soumith Chintala, Dhruv Batra, Jitendra Malik, and Devendra Singh Chaplot. Navigating to objects in the real world. *Science Robotics*, 8(79):eadf6991, 2023. 3
- [9] Abhinav Gupta, Adithyavairavan Murali, Dhiraj Prakashchand Gandhi, and Lerrel Pinto. Robot learning in homes: Improving generalization and reducing dataset bias. *Advances in neural information processing systems*, 31, 2018. 9
- [10] Yining Hong, Haoyu Zhen, Peihao Chen, Shuhong Zheng, Yilun Du, Zhenfang Chen, and Chuang Gan. 3d-llm: Injecting the 3d world into large language models. In *Thirty-seventh Conference on Neural Information Processing Systems*, 2023. 3
- [11] Nidhi Kalra, Dave Ferguson, and Anthony Stentz. Incremental reconstruction of generalized voronoi diagrams on grids. *Robotics and Autonomous Systems*, 57(2):123–128, 2009. 5
- [12] Mukul Khanna, Yongsan Mao, Hanxiao Jiang, Sanjay Haresh, Brennan Shacklett, Dhruv Batra, Alexander Clegg, Eric Undersander, Angel X. Chang, and Manolis Savva. Habitat synthetic scenes dataset (hssd-200): An analysis of 3d scene scale and realism tradeoffs for objectgoal navigation, 2023. 2, 9
- [13] Alexander Kirillov, Eric Mintun, Nikhila Ravi, Hanzi Mao, Chloe Rolland, Laura Gustafson, Tete Xiao, Spencer Whitehead, Alexander C. Berg, Wan-Yen Lo, Piotr Dollár, and Ross Girshick. Segment anything. *arXiv:2304.02643*, 2023. 4
- [14] Jacob Krantz, Erik Wijmans, Arjun Majumdar, Dhruv Batra, and Stefan Lee. Beyond the nav-graph: Vision-and-language navigation in continuous environments. In *Computer Vision—ECCV 2020: 16th European Conference, Glasgow, UK, August 23–28, 2020, Proceedings, Part XXVIII 16*, pages 104–120. Springer, 2020. 3
- [15] Jacob Krantz, Aaron Gokaslan, Dhruv Batra, Stefan Lee, and Oleksandr Maksymets. Waypoint models for instruction-guided navigation in continuous environments. In *Proceedings of the IEEE/CVF International Conference on Computer Vision*, pages 15162–15171, 2021. 3
- [16] Obin Kwon, Jeongho Park, and Songhwai Oh. Renderable neural radiance map for visual navigation. In *Proceedings of the IEEE/CVF Conference on Computer Vision and Pattern Recognition*, pages 9099–9108, 2023. 3
- [17] Junnan Li, Dongxu Li, Caiming Xiong, and Steven Hoi. Blip: Bootstrapping language-image pre-training for unified vision-language understanding and generation. In *International Conference on Machine Learning*, pages 12888–12900. PMLR, 2022. 6
- [18] Lin Li, Xinkai Zuo, Huixiang Peng, Fan Yang, Haihong Zhu, Dalin Li, Jun Liu, Fei Su, Yifan Liang, and Gang Zhou. Improving autonomous exploration using reduced approximated generalized voronoi graphs. *Journal of Intelligent & Robotic Systems*, 99:91–113, 2020. 3
- [19] Junjia Liu, Jianfei Guo, Zehui Meng, and Jingtao Xue. Revolt: Relational reasoning and voronoi local graph planning for target-driven navigation. *arXiv preprint arXiv:2301.02382*, 2023. 3
- [20] Shilong Liu, Zhaoyang Zeng, Tianhe Ren, Feng Li, Hao Zhang, Jie Yang, Chunyuan Li, Jianwei Yang, Hang Su, Jun Zhu, et al. Grounding dino: Marrying dino with grounded pre-training for open-set object detection. *arXiv preprint arXiv:2303.05499*, 2023. 4
- [21] Arjun Majumdar, Gunjan Aggarwal, Bhavika Suresh Devnani, Judy Hoffman, and Dhruv Batra. ZSON: Zero-shot object-goal navigation using multimodal goal embeddings. In *Advances in Neural Information Processing Systems*, 2022. 1, 2
- [22] OpenAI. Gpt-4 technical report, 2023. 9
- [23] Long Ouyang, Jeff Wu, Xu Jiang, Diogo Almeida, Carroll L. Wainwright, Pamela Mishkin, Chong Zhang, Sandhini Agarwal, Katarina Slama, Alex Ray, John Schulman, Jacob Hilton, Fraser Kelton, Luke Miller, Maddie Simens, Amanda Askell, Peter Welinder, Paul Christiano, Jan Leike, and Ryan Lowe. Training language models to follow instructions with human feedback, 2022. 2, 9
- [24] Jeongeun Park, Taerim Yoon, Jejoon Hong, Youngjae Yu, Matthew Pan, and Sungjoon Choi. Zero-shot active visual search (zavis): Intelligent object search for robotic assistants. In *2023 IEEE International Conference on Robotics and Automation (ICRA)*, pages 2004–2010, 2023. 1
- [25] Alec Radford, Jeffrey Wu, Rewon Child, David Luan, Dario Amodei, Ilya Sutskever, et al. Language models are unsupervised multitask learners. *OpenAI blog*, 1(8):9, 2019. 9
- [26] Santhosh K Ramakrishnan, Aaron Gokaslan, Erik Wijmans, Oleksandr Maksymets, Alex Clegg, John Turner, Eric Undersander, Wojciech Galuba, Andrew Westbury, Angel X Chang, et al. Habitat-matterport 3d dataset (hm3d): 1000

large-scale 3d environments for embodied ai. *arXiv preprint arXiv:2109.08238*, 2021. 2

- [27] Santhosh K. Ramakrishnan, Devendra Singh Chaplot, Ziad Al-Halah, Jitendra Malik, and Kristen Grauman. Poni: Potential functions for objectgoal navigation with interaction-free learning. In *Computer Vision and Pattern Recognition (CVPR), 2022 IEEE Conference on*. IEEE, 2022. 3
- [28] James A Sethian. A fast marching level set method for monotonically advancing fronts. *proceedings of the National Academy of Sciences*, 93(4):1591–1595, 1996. 7
- [29] Dhruv Shah, Michael Equi, Blazej Osinski, Fei Xia, Brian Ichter, and Sergey Levine. Navigation with large language models: Semantic guesswork as a heuristic for planning. In *7th Annual Conference on Robot Learning*, 2023. 3
- [30] Stefan Van der Walt, Johannes L Schönberger, Juan Nunez-Iglesias, François Boulogne, Joshua D Warner, Neil Yager, Emmanuelle Gouillart, and Tony Yu. scikit-image: image processing in python. *PeerJ*, 2:e453, 2014. 4
- [31] Karmesh Yadav, Santhosh Kumar Ramakrishnan, John Turner, Aaron Gokaslan, Oleksandr Maksymets, Rishabh Jain, Ram Ramrakhya, Angel X Chang, Alexander Clegg, Manolis Savva, Eric Undersander, Devendra Singh Chaplot, and Dhruv Batra. Habitat challenge 2022. <https://aihabitat.org/challenge/2022/>, 2022. 9
- [32] Brian Yamauchi. A frontier-based approach for autonomous exploration. In *Proceedings 1997 IEEE International Symposium on Computational Intelligence in Robotics and Automation CIRA'97.'Towards New Computational Principles for Robotics and Automation'*, pages 146–151. IEEE, 1997. 8, 9
- [33] Bangguo Yu, Hamidreza Kasaei, and Ming Cao. Co-navgpt: Multi-robot cooperative visual semantic navigation using large language models, 2023. 3
- [34] Bangguo Yu, Hamidreza Kasaei, and Ming Cao. L3mvn: Leveraging large language models for visual target navigation. *arXiv preprint arXiv:2304.05501*, 2023. 3, 8, 9
- [35] Qianfan Zhao, Lu Zhang, Bin He, Hong Qiao, and Zhiyong Liu. Zero-shot object goal visual navigation. In *2023 IEEE International Conference on Robotics and Automation (ICRA)*, pages 2025–2031, 2023. 1
- [36] Kaiwen Zhou, Kaizhi Zheng, Connor Pryor, Yilin Shen, Hongxia Jin, Lise Getoor, and Xin Eric Wang. Esc: Exploration with soft commonsense constraints for zero-shot object navigation. *arXiv preprint arXiv:2301.13166*, 2023. 2, 3, 8, 9